41th ERF, September 1–4, 2015, Munich, Germany
022

Measurement of the Rotor Blade Section Aerodynamic Coefficients by Particle Image Velocimetry

A. Zanotti*[1], G. Gibertini[1], F. Auteri[1], G. Campanardi[1], G. Droandi[1], D. Grassi[1] and G. Crosta[2]

[1]Politecnico di Milano – Dipartimento di Scienze e Tecnologie Aerospaziali
Via La Masa 34, 20156 Milano – Italy
[2]Agusta Westland – HSD Department
via G.Agusta 520, Cascina Costa di Samarate (VA) – Italy
e–mail: *alex.zanotti@polimi.it

Keywords: Particle Image Velocimetry, Rotor, Wind Tunnel, Aerodynamic Loads.

Abstract

Particle Image velocimetry surveys were carried out around the blade section at 65% radius of a four-bladed articulated rotor model to evaluate the airloads coefficients from velocity data. The blade section aerodynamic loads were calculated using the control volume approach and compared with the results of the blade element momentum theory in hovering for validation. As the compressibility effects for the present test case are not negligible, the pressure on the contour of the control surface was computed from the measured local velocity using the isentropic relations. The vertical force coefficient calculated from PIV data shows a quite good agreement with blade element theory results. The experimental campaign included also surveys around the blade section equipped with passive Gurney flap with different height. Thus, the method to obtain the aerodynamic loads from PIV data was employed to evaluate the effect of the flap on the vertical aerodynamic force acting on the blade section in hovering.

Nomenclature

$BEMT$	blade element momentum theory
C_{F_z}	vertical force coefficient
C_T	rotor thrust coefficient
dF_z	vertical force on blade section [N/m]
h	Gurney flap height
Ma	Mach number
p	pressure [Pa]
PIV	Particle Image Velocimetry
R	rotor radius [m]
Re	Reynolds number
s	abscissa on the integration contour [m]
u	horizontal velocity component [m/s]
$\|U\|$	velocity magnitude [m/s]
U_∞	free-stream velocity [m/s]
X	horizontal coordinate [m]
Y	span-wise coordinate [m]
Z	vertical coordinate [m]
α	angle of attack [deg]
σ	rotor solidity
ψ	azimuthal blade angle [deg]
θ	blade pitch angle at 75% R [deg]
ω	rotor rotational speed [RPM]

1 Introduction

Measuring the aerodynamic loads acting on a rotor-model blade section represents a challenging task. In fact, the limited dimensions of the blade model make difficult to install a proper number of miniature pressure transducers around the airfoil contour to obtain an accurate evaluation of the airloads coefficients by integrating the pressure distribution. Therefore, the possibility of calculating the blade section aerodynamic loads from velocity data represents a very interesting possibility.

The activity described in the paper was carried out in the frame of GUM Research Project, being part of the Green Rotorcraft Integrated Technology Demonstrator of the Clean Sky programme, co-funded by the European Commission. The main scope of the present work was the evaluation of the airloads coefficients over a rotor-blade section. In the present activity, 2C PIV surveys were carried out around the blade section at 65% radius of a four-bladed articulated rotor model of AgustaWestland [1]. The test activity was performed in the open test section of Politecnico di Milano large wind tunnel and included surveys both on the upper and lower surface of the blade section airfoil to obtain the velocity data around the entire airfoil contour. The blade section aerodynamic coefficients were calculated using the control volume approach [2] and compared with the results of the blade element momentum theory in hovering [3]. In particular, in order to calculate the vertical force coefficient representing the main goal of the activity, pressure on the integration contour of the control surface was calculated using the isentropic equations under the assumptions that in the outer region of the measurement window the flow behaves as adiabatic and inviscid [4].

PIV measurements were carried out also around the same section of the blade equipped with a passive Gurney flap positioned on the lower surface of the airfoils. The investigation of the effect of Gurney flaps on blade aerodynamic performance represents an important topic in rotorcraft aerodynamics research field [5, 6]. With this aim, the effect of Gurney flaps of different height was evaluated by comparison of the vertical aerodynamic force coefficients computed from PIV data measured in the same hovering condition.

2 Experimental Set Up

The four-bladed fully articulated rotor was set up in the open test section of the large wind tunnel of Politecnico di Milano (see Fig. 1). The rotor model is equipped with a strain gauge six-components balance to measure the aerodynamic loads and moments.

The blades in carbon fiber were built with a 90 mm constant chord, 8° linear twist and a constant NACA 0012 section. The rotor radius is equal to 1.1 m. A passive Gurney flap with different height (h = 1.5 mm, h = 2 mm and h = 2.5 mm) can be attached to the lower surface at radial stations between 55.5% and 69.5% of the rotor radius. The Gurney flap vertical to the chord is located at 95% of the airfoil chord. The blade surface around the 65% of the radius, corresponding to the section selected for PIV surveys, was painted with black opaque paint to reduce laser reflections.

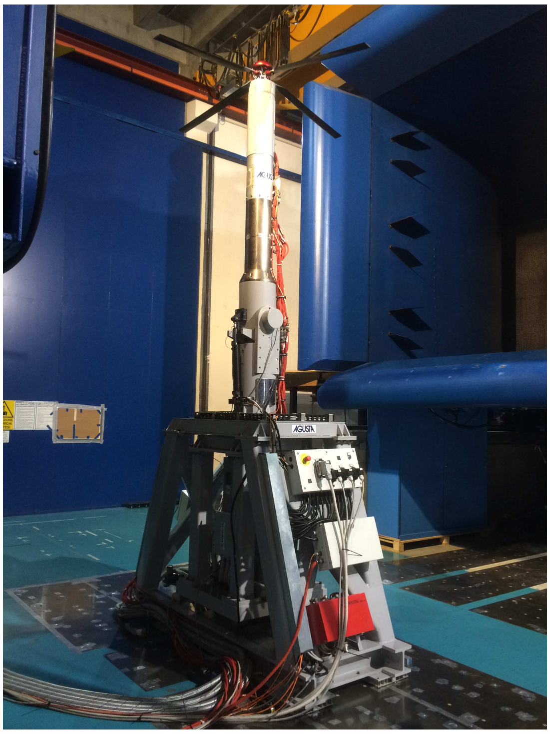

Figure 1: AgustaWestland rotor model in the open test section of Politecnico di Milano large wind tunnel.

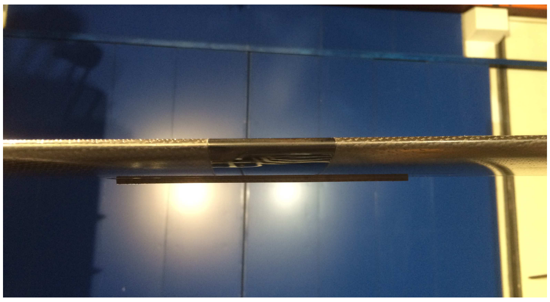

Figure 2: Particular of the carbon fiber blade equipped with passive Gurney flap (h = 2.5 mm).

2.1 PIV set up

The employed PIV system comprises a Nd:Yag double pulsed laser with 200 mJ output energy and a wavelength of 532 nm and a double shutter CCD camera with a 12 bit, 1952 $\times$ 1112 pixel array equipped with a 105 mm lens. Two-components PIV surveys were carried out over a measurement window that spans more than the entire chord of the blade section at the 65% of the rotor radius. The velocity field around the entire blade section contour was reconstructed from PIV surveys carried out both on the upper and lower surface of the airfoil. The dimensions of the complete measurement window around the blade section are 135 mm $\times$ 90 mm. For the survey over the airfoil upper surface the laser was mounted on a metallic structure attached to the overhead crane of the wind tunnel building. On the other hand, the survey over the airfoil lower surface were carried out with the metallic structure supporting the laser positioned on the floor. The laser was mounted horizontally on the metallic structure as the optics is equipped with a mirror for adjusting the laser sheet to be orthogonal to the blade axis. The camera was mounted on a metallic structure made of aluminium profiles. The pitch angle of the camera can be adjusted according to the cone angle of the rotor. The layout of the PIV instrumentation for the airfoil upper surface survey is shown in Fig. 3.

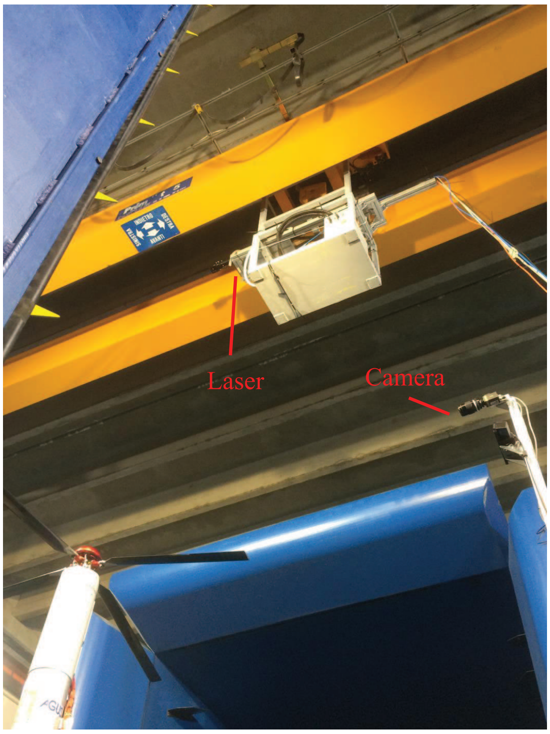

Figure 3: PIV instrumentation set up for the surveys on the blade section upper surface.

A particle generator with Laskin nozzles was positioned on the overhead crane for the flow insemination. The tracer particles, consisting in small oil droplets with a diameter within the range of 1-2 μm. A total amount of 200 image pairs were acquired for each test condition. The acquisition of the image pairs was phase-locked with the azimuthal angle of the master blade selected for the test. The image pairs post-processing was carried out using the PIVview 2C software [7] of PIVTEC. Multigrid technique [8] was employed to correlate the image pairs, up to an interrogation window of 32 $\times$ 32 pixels.

3 Pressure field

Pressure on the integration contour of the control surface considered for the calculation of the aerodynamic loads was computed from the measured local velocity using the isentropic relations [9]. In particular, considering that in the outer region of the measurement window the flow can be assumed to behave as adiabatic and inviscid, pressure on the contour of the control surface was computes as

$$\frac{p}{p_\infty} = \left(1 + \frac{\gamma - 1}{2} M_\infty^2 \left(1 - \frac{U^2}{U_\infty^2}\right)\right)^{\frac{\gamma}{\gamma-1}} \quad (1)$$

where U is the velocity magnitude. A more general method for incompressible flow conditions was developed to reconstruct the pressure field from measured velocity data. This method, based on a generalization of the Glowinski-Pironneau method for the uncoupled solution of the incompressible Navier-Stokes equations, can be used for applications where the isentropic flow assumptions are not valid and was successfully employed to compute pressure field from phase-averaged and time-resolved PIV data set measured around the upper surface of a pitching airfoil at low Mach number [10]. This method was not applied in the present work as the compressibility effects for the considered test case are not negligible.

4 Validation of the calculated aerodynamic coefficient

In order to validate the calculation of the aerodynamic coefficients from PIV data, a classical blade element momentum theory (BEMT) approach was used to calculate the distribution of the aerodynamic loads along the blade span for the selected test condition in hovering. Even though this aerodynamic model is very simple, it is mathematically parsimonious [11] and suitable to predict well the performance of helicopter rotor.

Moreover, a two-dimensional CFD simulation was carried out with a compressible Navier-Stokes solver using the angle of attack and the free-stream flow conditions (Reynolds and Mach numbers) predicted by the BEMT solver in correspondence of the blade section investigated by PIV. The simulation results were useful to achieve an insight about the level of confidence on the pressure computed over the integration contour as well as on the measured velocity field for the investigated test case.

4.1 BEMT solver

The BEMT aerodynamic solver [12] employed a physico-mathematical rotor model which is based on a combination of the simple momentum theory with the classical blade element theory. This approach, that implies the assumption of an axisymmetrical flow, can be efficiently used to predict the rotor performance both in hovering and in axial flight. In order to improve results quality, swirl velocity effects were also taken into account and, furthermore, the Prandtl's tip loss correction was applied. The airfoil data necessary to the BEMT solver were previously stored in tables for a wide range of angles of attack, Reynolds and Mach numbers, combining wind tunnel data [13] and two-dimensional CFD results performed with the ROSITA solver. In the present work, the performance of the rotor blades for the prescribed test condition was computed considering the measured rotor thrust as trim requirement.

4.2 CFD solver

The CFD code ROSITA [14] numerically integrates the unsteady compressible RANS equations coupled with the one-equation turbulence model of Spalart-Allmaras. The Navier-Stokes equations are formulated in terms of the absolute velocity and are discretised in space by means of a cell-centred finite-volume implementation of Roe's scheme. Second order accuracy is obtained through the use of MUSCL extrapolation supplemented with a modified version of the Van Albada limiter introduced by Venkatakrishnan. Time advancement is carried out with a dual-time formulation, employing a 2^{nd} order backward differentiation formula to approximate the time derivative and a fully unfactored implicit scheme in pseudo-time. The generalised conjugate gradient (GCG), in conjunction with a block incomplete lower-upper preconditioner, is used to solve the resulting linear system.

For the simulation of the blade section condition investigated by PIV, a structured multiblock two-dimensional C-grid was built for the NACA 0012 airfoil with a total number of about 125000 hexaedral elements. The first layer of elements near the airfoil surface was set to obtain a value of the dimensionless wall distance $y+ = 1$. This value is based on the flow conditions estimated by the BEMT analysis for the investigated test condition. A view of the employed grid close to the airfoil is shown in Fig. 4 together with the reference system used in the work.

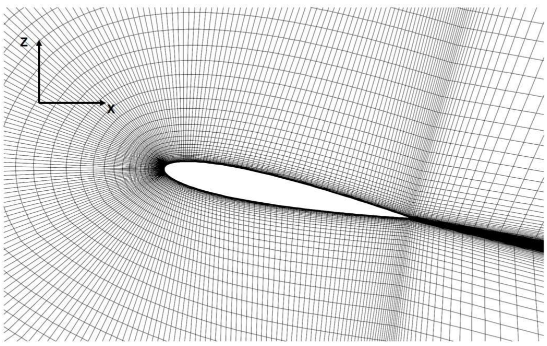

Figure 4: Two-dimensional grid for the NACA 0012 blade section with the reference system.

5 Results

The rotational speed of the rotor during the tests was set to $\omega = 1600$ RPM. The hovering tests included the clean blade as well as the configuration with the three different Gurney flaps. PIV results are presented for the test condition with commanded collective angle of 13 degrees. Table 1 presents the blade pitch angle measured at 75% of the rotor radius for the selected PIV test configurations.

Blade	θ **[deg]**
Clean	12
Gurney $h = 1.5$ mm	11.8
Gurney $h = 2$ mm	11.8
Gurney $h = 2.5$ mm	11.7

Table 1: Measured blade pitch angle for PIV tests in hovering.

The PIV measurements were performed in hovering conditions at the azimuthal blade angle $\psi = 270°$. The phase-averaged velocity fields are presented according to the blade section reference system X-Y-Z. In the PIV velocity fields the region close to the airfoil influenced by reflections is blanked.

Figure 5 shows the contours of the phase-averaged horizontal velocity component u measured by PIV for the clean blade. The PIV flow field was compared to the velocity field computed by CFD simulation carried out using the angle of attack and the flow conditions estimated by the BEMT analysis for the investigated blade section ($Re = 7.3 \cdot 10^5$, $Ma = 0.349$). An overall quite good agreement of the velocity field can be observed with only exception of the airfoil wake. This discrepancy could be related to the PIV measurement resolution that is insufficient to describe the velocity defect in the thin wake of the airfoil. This feature influences the calculation of the aerodynamic tangential force that, therefore, is not presented in the paper.

The vertical force was calculated using the Navier-Stokes momentum equation in the integral form [2, 4]. The integration contour employed is depicted in Fig. 5(a). Viscous stresses along the contour of the control surface were neglected as their contribution to the calculation of the vertical force coefficients were negligible, while turbulent stresses obtained from the measured velocity fluctuations were considered in the calculation. The comparison between the pressure on the integration contour computed from PIV data using the isentropic equations and from CFD simulation is presented in Fig. 6, where s is the abscissa on the integration contour. A good agreement is found from this comparison, showing that for the present case a good level accuracy of

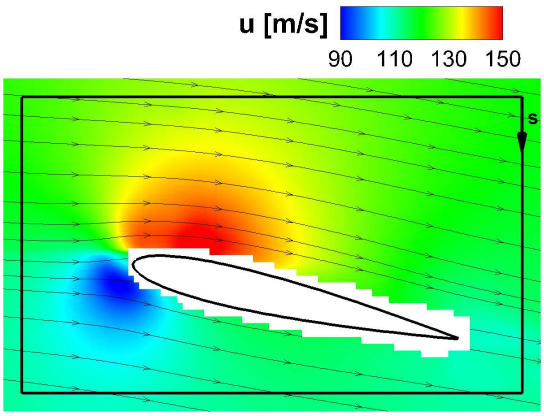

(a) PIV

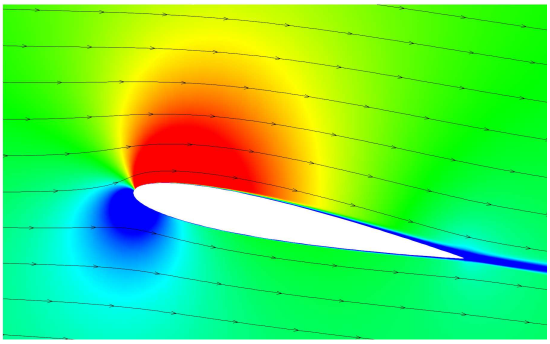

(b) CFD

Figure 5: Comparison of the PIV and CFD velocity fields for the clean blade section.

the pressure computation is obtained using the isentropic equations.

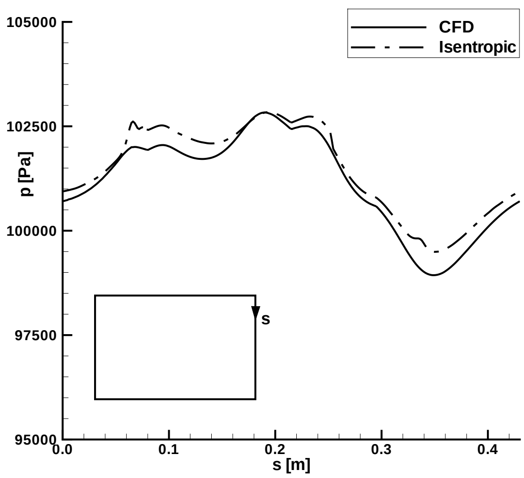

Figure 6: Pressure comparison on the contour of the control surface: pressure computed from PIV data using the isentropic equations and from CFD simulation.

Figure 7 shows the distribution of the vertical aerodynamic force along the blade span computed by BEMT solver for the investigated hovering condition. In particular, the value of the vertical force acting on the blade section at 65% of the rotor radius is indicated by dashed lines.

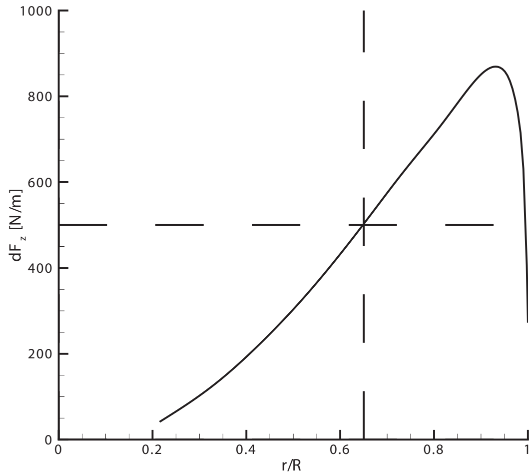

Figure 7: Distribution of the vertical aerodynamic force along the blade span computed by BEMT.

The vertical aerodynamic force coefficient calculated from PIV data on the investigated blade section is compared with the value computed by the BEMT analysis in Tab. 2.

	from PIV	**BEMT**	**Error** [%]
C_{F_z}	0.607	0.635	4.4

Table 2: Comparison of the C_{F_z} calculated from PIV data with BEMT for the clean blade section at 65%R.

The discrepancy between the vertical force coefficient computed from PIV data and the BEMT analysis results is in the order of few percents. Thus, the employed method shows a good level of accuracy for the calculation of the vertical aerodynamic force for the present hovering condition. The method was therefore applied to the PIV measurements carried out around the blade section equipped with the Gurney flaps to evaluate the performance of the flaps with different height with respect to the clean condition for the same commanded collective angle (see Tab. 1).

Figure 8 shows the contours of the phase-averaged horizontal velocity component u measured by PIV for the blade section configurations with the different Gurney flaps.

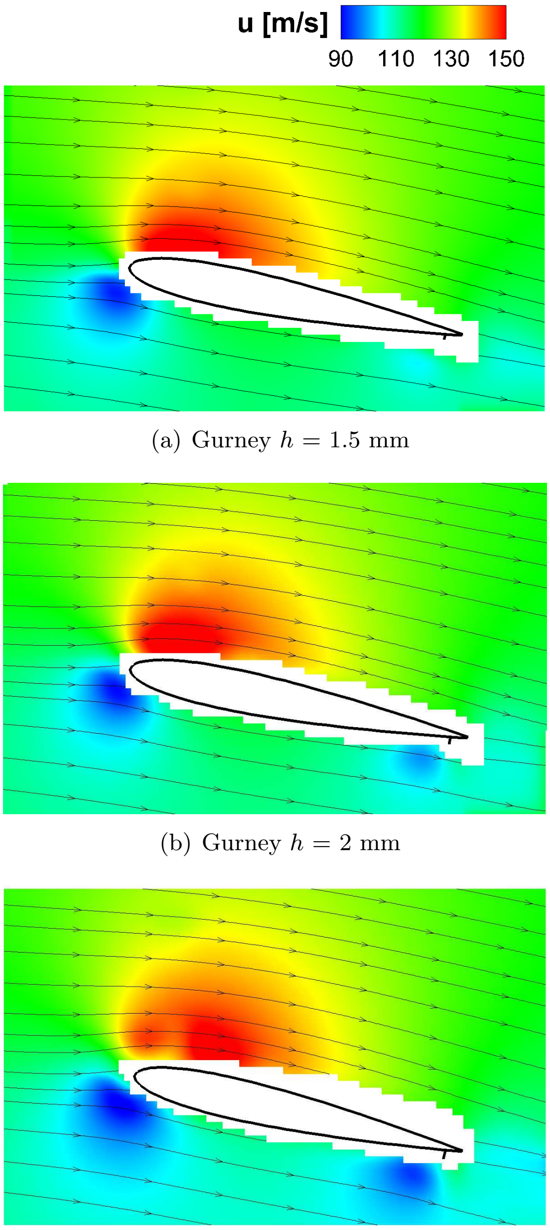

(a) Gurney h = 1.5 mm

(b) Gurney h = 2 mm

(c) Gurney h = 2.5 mm

Figure 8: Comparison of the PIV velocity fields for the blade section equipped with Gurney flaps.

The effect of the Gurney flap is apparent from the measured velocity flow field. In particular, a further decrease of the velocity in the flow region around the Gurney flap can be observed increasing the height of the Gurney flap.

Figure 9 shows the vertical aerodynamic force coefficient calculated from PIV data for the blade section equipped with the different Gurney flaps compared with the one computed for the clean blade section geometry. In particular, the percentual increase of the vertical force coefficient with respect to the clean geometry is reported in the figure.

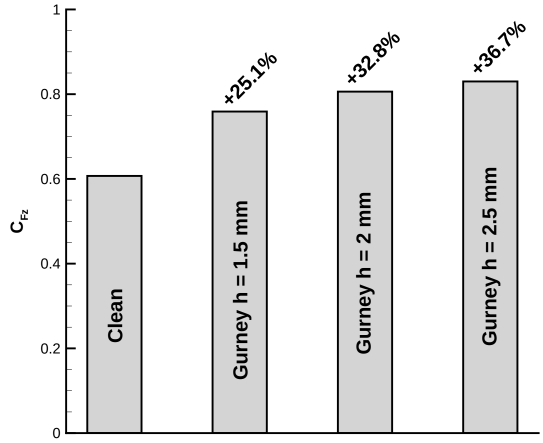

Figure 9: Comparison of the C_{F_z} calculated from PIV data for the blade section at 65%R with and without the Gurney flaps.

An apparent increase of the vertical force coefficient was computed for the blade section configuration equipped with the different Gurney flaps with respect to the clean geometry for this hovering test condition. In particular, as it can be expected, the computed C_{F_z} is higher increasing the Gurney flaps height [5]. The good level of confidence of this computed trend is confirmed by the comparison of the rotor thrust coefficient measured in hovering for the different blade configurations shown in Fig. 10.

6 Conclusions

An experimental activity involving the use of PIV surveys around the blade section of a rotor model was carried out to evaluate the aerodynamic loads from velocity data measured in hovering. The vertical force coefficient acting on the blade section at 65% of the rotor radius was calculated using the control volume approach. With this aim, pressure on the integration contour was calculated from the measured local velocity using the isentropic relations. The method was validated by compar-

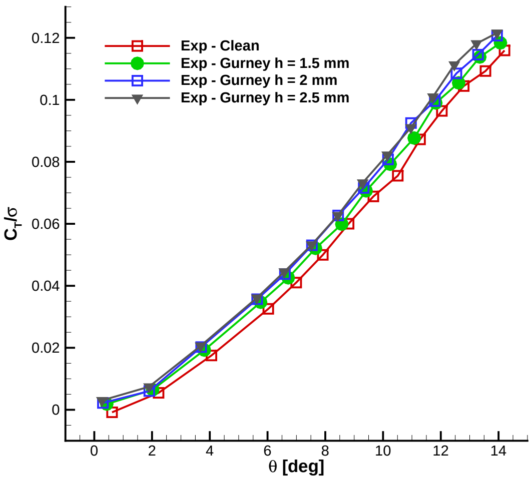

Figure 10: Comparison of the C_T/σ measured by the rotor balance with and without the Gurney flaps in hovering, $\omega = 1600$ RPM.

ison of the computed vertical force coefficient with a blade element momentum theory analysis carried out for the selected test condition. Thus, the method was applied to PIV measurement carried out around the same blade section equipped with Gurney flaps with different height to evaluate their effects on the blade performance in hovering. An apparent increase of about 37% of the vertical force coefficient was found for the configuration with the highest Gurney flap tested with respect to the clean blade section geometry.

Acknowledgements

The research leading to these results has received funding from the European Community's Seventh Framework Programme (FP7/2007-2013) for the Clean Sky Joint Technology Initiative under grant agreement n. 298192.

References

[1] Biava M, Campanardi G, Gibertini G, Grassi D, Vigevano L, Zanotti A. Wind Tunnel Open Section Characterization for Rotorcraft Tests, 38th European Rotorcraft Forum, Amsterdam, the Netherlands, 4-7 September 2012.

[2] Anderson JD. *Fundamentals of Aerodynamics*. McGraw-Hill, New York, 2nd edn, 1991.

[3] Leishman JG. *Principles of helicopter aerodynamics*. Cambridge University Press, 2006.

[4] Ragni D, Ashok A, van Oudheusden BW and Scarano F. Surface pressure and aerodynamic loads determination of a transonic airfoil based on particle. *Measurement, Science and Technology*, Vol. 20, 074005, pp. 1-14, 2009.

[5] Yee K, Joo W and Lee DH. Aerodynamic performance analysis of a gurney flap for rotorcraft application. *Journal of Aircraft*, Vol. 44, pp 1003-1014, 2007.

[6] Zanotti A, Grassi D and Gibertini G. Experimental Investigation of a Trailing Edge L-shaped Tab on a Pitching Airfoil in Deep Dynamic Stall Conditions. *Proceedings of the Institution of Mechanical Engineers, Part G: Journal of Aerospace Engineering*, Vol. 228, N. 12, pp 2371-2382, 2014.

[7] PIVview 2C/3C, User Manual, PIVTEC, www.pivtec.com, 2010.

[8] Raffel M., Willert C., Wereley S. and Kompenhans J. Particle Image Velocimetry - A Practical Guide, Springer Verlag, Berlin, 2007.

[9] Anderson JD. *Modern Compressible Flow with Historical Perspective*. McGraw-Hill, New York, 3rd edn, 2003.

[10] Auteri F, Carini M, Montagnani D, Zagaglia D, Merz CB, Gibertini G and Zanotti A. A novel approach for reconstructing pressure from PIV velocity measurements. *Experiments in Fluids*, Vol. 56 , N. 45, pp 1-16, 2015.

[11] Leishman JG and Rosen KM. Challenges in the Aerodynamic Optimization of High-Efficiency Proprotors. *Journal of the American Helicopter Society*, Vol. 56:012004, N. 1, pp 1-21, 2011.

[12] Droandi G and Gibertini G. Aerodynamic Blade Design With Multi-Objective Optimization For A Tiltrotor Aircraft. *Aircraft Engineering and Aerospace Technology*, Vol. 87, N. 1, pp 19-29, 2015.

[13] Abbott IH and Von Doenhoff AE. *Theory of Wing Sections, Including a Summary of Airfoil Data*. Dover Publications, New York, 1959.

[14] Biava M. RANS computations of rotor/fuselage unsteady interactional aerodynamics. PhD thesis, Politecnico di Milano, 2007.